

Physical, Chemical and Optical Properties of Fine Aerosol as a Function of Relative Humidity at Gosan, Korea during ABC-EAREX 2005

Kwang-Joo Moon^{1),2)}, Jin-Seok Han^{1):*} and Seog-Yeon Cho²⁾

¹⁾Department of Air Quality Research, Climate and Air Quality Research Division, National Institute of Environmental Research, Environmental Research Complex, Kyeongseo-dong, Seo-gu, Incheon 404-170, Korea

²⁾Department of Environmental Engineering, Inha University, Yonghyeon-dong, 253, Incheon, Korea

*Corresponding author. Tel: +82-32-560-7250, E-mail: nierhan@korea.kr

ABSTRACT

The water uptake by fine aerosol in the atmosphere has been investigated at Gosan, Korea during ABC-EAREX 2005. The concentration of inorganic ion and carbon components, size distribution, and light scattering coefficients in normal and dry conditions were simultaneously measured for PM_{2.5} by using a parallel integrated monitoring system. The result of this study shows that ambient fine particles collected at Gosan were dominated by water-soluble ionic species (35%) and carbonaceous materials (18%). In addition, it shows the large growth of aerosol in the droplet mode when RH is higher than 70%. Size distribution of the particulate surface area in a wider size range (0.07-17 μm) shows that the elevation of RH make ambient aerosol grow to be the droplet mode one around 0.6 μm or the coarse mode one, larger than 2.5 μm. Hygroscopic factor data calculated from the ratio of aerosol scattering coefficients at a given ambient RH and a reference RH (25%) show that water uptake began at the intermediate RH range, from 40% to 60%, with the average hygroscopic factor of 1.10 for 40% RH, 1.11 for 50% RH, and 1.17 for 60% RH, respectively. Finally, average chemical composition and the corresponding growth curves were analyzed in order to investigate the relationship between carbonaceous material fraction and hygroscopicity. As a result, the aerosol growth curve shows that inorganic salts such as sulphate and nitrate as well as carbonaceous materials including OC largely contribute to the aerosol water uptake.

Key words: PM_{2.5}, Size distribution, Hygroscopic growth, Growth curve, Scattering coefficient

1. INTRODUCTION

Recently, INDOEX revealed the so-called “brown cloud” phenomenon over the Northern Indian Ocean region with a large impact on the solar radiative heating of the region. The result suggests that urban haze can spread over an entire sub-continent and an ocean basin due to the long-range transport and finally could perturb the radiative energy budget of the region and global climate (Ramanathan *et al.*, 2001). In this point of view, Northeast Asia has attracted much attention due to its increasingly high emission of anthropogenic air pollutants. An international program entitled Asian Brown Cloud (ABC) started in Asia in 2002 in order to understand the effects of air pollution and mineral dust in this region on the earth’s climate and environment (Ramanathan and Crutzen, 2003). This study presents the result of ABC-EAREX 2005 conducted in the spring monsoon season at Gosan super site.

Previous works during INDOEX found that the brownish haze which is widely spread over the Asian continents consists of a mixture of anthropogenic sulfate, nitrate, organics, black carbon, dust and fly ash particles, and natural aerosols such as sea salt and mineral dust (Quinn *et al.*, 2002). Generally, inorganic salts and carbonaceous aerosols may play an important role in radiative and climate forcing. Especially, particulate sulfate, nitrate, organic carbon, soil, and size distribution have been potentially associated with light-scattering of solar radiation (Sisler and Malm, 2000). In addition, the uptake and loss of water by aerosols according to the ambient relative humidity can significantly change not only the size distribution and chemical composition, but also the light scattering properties of aerosol (Tang, 1996). Many laboratory and field studies have been performed to understand the relationship among the hygroscopicity, physi-

cal, chemical, and optical properties of ambient aerosols. However, there is still a need for further examination of the hygroscopic nature of ambient aerosols and the impact of aerosol growth by water uptake on radiation transfer through the atmosphere. For example, organic compounds also contribute significantly to the fine aerosol although water-soluble inorganic salts often contribute the largest part of PM mass. Throughout Northeast Asia, organic carbon contributes between 13% and 23% of the fine particle mass ($D_p < 2.5 \mu\text{m}$) with the highest fractions occurring at the major industrial regions located in Northeast China (Han *et al.*, 2006; Han *et al.*, 2004). At this time, the polar organic carbon compounds such as carbonyl groups which consist of organic carbon can also contribute to water uptake by the ambient aerosol (Day and Malm, 2001). However, the roles of most other organic carbon compounds playing in the water uptake of ambient aerosol were not much known while inorganic salts and their hygroscopic properties have been studied comprehensively.

In several previous works, the water uptake by ambient aerosols was investigated by using the Tandem Differential Mobility Analyzer (TDMA) (Day and Malm, 2001; Dick *et al.*, 2000; Swietlicki *et al.*, 1999; McMurry and Stolzenburg, 1998). The instrument consists of the sampling inlet assembled with $\text{PM}_{2.5}$ size cut cyclone, RH control part, and nephelometer coupled with RH and temperature sensors. In this study, the similar structure was organized in a parallel integrated monitoring system. The newly organized system measures the change of particle size in parallel while the existing TDMA is made up of a serial system. This system simultaneously measures the size distribution of ambient aerosol, and light scattering coefficients in dry and normal conditions. The results are expected to help us to understand the characteristics of ambient hygroscopic aerosol and their complicated growth behaviour at Gosan, Korea, which is a representative background site in Northeast Asia during ABC-EAREX 2005.

2. DESCRIPTION OF THE MONITORING

Aerosol monitoring was performed at Gosan, Jeju Island, Korea ($33^\circ 17' \text{N}$, $126^\circ 10' \text{E}$, 70 m a.s.l) during ABC-EAREX 2005 intensive measurement periods, from 8 March to 6 April 2005. Gosan has served as a super site of ABC project, which is an ideal location for studying the long-range transport of air pollutants in Northeast Asia as shown in Fig. 1. In this region, continentally derived aerosol may be transported to the

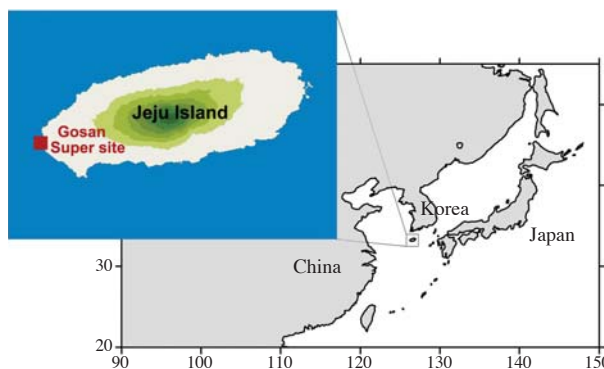


Fig. 1. Location of Gosan super site.

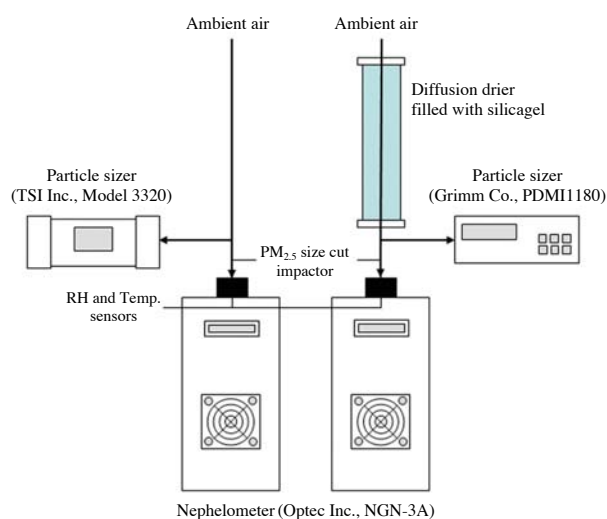
leeward of prevailing westerlies in spring. The aerosols originated in continents contain not only soil dust such as Asian dust, but also anthropogenic pollutants involved with fossil fuel combustion, industrial processes, biomass/biofuel burning, and so on (Han *et al.*, 2005). In addition, they can mix and chemically interact with marine aerosol components such as sea salt, biogenically derived sulfates and carbonaceous species during the transportation. During the measurement period, two Asian dust outbreaks were observed from 17 to 18 March and on 29 March. In this study, aerosol data during Asian dust periods were not analyzed.

2.1 Real-time Monitoring of Particulate Chemical Composition

The mass and chemical composition of $\text{PM}_{2.5}$ was continuously monitored with the interval of 1 hour. Anderson FH-62 using β -ray attenuation method was operated to measure $\text{PM}_{2.5}$ mass concentration. The real-time monitoring of water-soluble inorganic ions such as SO_4^{2-} , NO_3^- , Cl^- , NH_4^+ , Na^+ , K^+ , Ca^{2+} , and Mg^{2+} was conducted by using an Ambient Ion Monitor (AIM) (URG-9000B, URG Co.). The configuration of the AIM and the operating condition is described in the previous work (Moon *et al.*, 2006) and is summarized as follows: in a liquid diffusion denuder, interfering acid gases in sample air are preferentially removed. Then this system introduces atmospheric particle into a super-saturated environment by mixing the airflow with 100°C steam, which grow the particles into droplets large enough to be impacted in an inertial particle separator. The collected sample in a flowing liquid stream is analyzed by ion chromatography (Dionex, DX-100) connected with IonPac AS14A and CS12A column. The mass concentrations of thermal organic carbon (OC) and black carbon (BC) of $\text{PM}_{2.5}$ were thermally measured by semi-continuous carbon analyzer developed by Sunset Laboratory. The structure of the carbon monitor is basically the same

Table 1. Temperature profiles used for semi-continuous carbon analysis.

| Gas | Hold time (sec) | Temperature (°C) |
|-------------------|-----------------|------------------|
| He | 10 | No heating |
| He | 80 | 600 |
| He | 90 | 840 |
| He | 25 | No heating |
| He+O ₂ | 35 | 650 |
| He+O ₂ | 105 | 880 |
| CH ₄ | 120 | — |

**Fig. 2.** Schematic diagram of parallel integrated monitoring system.

as that described by Peterson and Richards (2002). The NIOSH 5040 method and involved gas TOT method were modified for stable field monitoring as summarized in Table 1. The validation of the used protocol has already done elsewhere (Arhami *et al.*, 2006).

2.2 Integrated Monitoring of Hygroscopic Properties

The hygroscopic and optical properties of ambient aerosols were measured by using a parallel integrated monitoring system which contains two nephelometers (NGN-3A, Optec Inc.) and two particle sizers (APS 3320, TSI Inc. and PDM 1108, Grimm, Co.). One set including a nephelometer and a particle sizer is operated in ambient conditions while the other dries the same aerosols to an RH of $25 \pm 5\%$ with a diffusion dryer. The hygroscopic factor for aerosol scattering, which is proposed on the basis of the optical parameters, is calculated as the ratio of the aerosol scattering coefficient at given RH to that at 25% RH. The existing TDMA which is arranged in series allows the selection of a single particle size in the first DMA. The par-

ticle size is measured in the second DMA after it has been exposed to increased or decreased relative humidity in a conditioner (Carrico *et al.*, 2005; Prenni *et al.*, 2003; Brechtel and Kreidenweis, 2000). On the other hand, the newly organized system parallel measures the particle size and scattering coefficient in normal and dry condition as shown in Fig. 2. This system consists of the sampling inlet, RH control part, particle sizer, and nephelometer coupled with RH and temperature sensors. Two nephelometers measured total scattering of PM_{2.5} at 550 nm. Impactors combined with the sample inlets of them allowed the collection of fine particles, aerodynamic diameter less than 2.5 μm. During the operation, continuous 2-minute integrations were conducted with a clean air calibration approximately every 27 hours. Particle sizers simultaneously count average number concentration of particles in more than 15 channels with 10-minute integration. The aerodynamic cut size is ranged from 0.5 to 20 μm.

3. RESULTS AND DISCUSSION

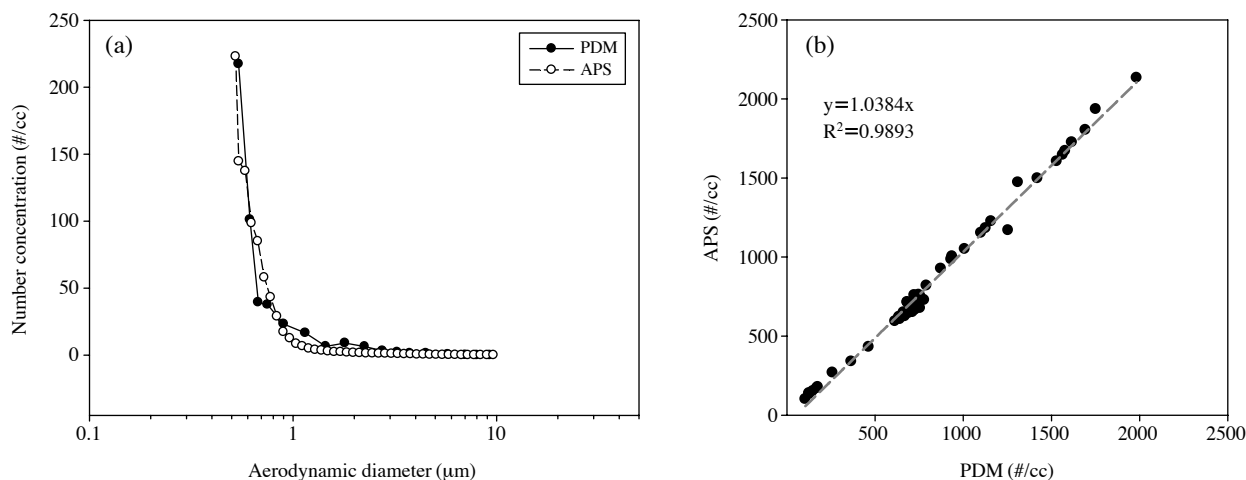
3.1 Quality Control

Moon *et al.* (2006) and Han *et al.* (2006b) discussed the agreement between these various measurement technologies as well as the measured chemical compositions of various aerosol species. It was found that the 24-hour bulk measurements agreed well with the semi-continuous measurements bias compared to the 24-hour average data. The filter-based data of nitrate and ammonium were lower than the results of real-time monitoring influenced by volatilization losses of ammonium salts in forms of NH₄Cl and NH₄NO₃ from aerosol matter during the storage. On the other hand, AIM-derived ion components showed similar concentration levels with another monitoring system, PILS-IC with less than 20% difference and good correlation ($R > 0.8$). The Sunset OC/EC data obtained through the modified NIOSH protocol was compared favorably with the in-situ measurements using the NIOSH 5040 method. On average, Sunset-derived TC showed about 6% difference between the two different protocols.

Oberreit *et al.* (2001) conducted comparison of the Grimm optical particle counter to the TSI aerodynamic particle sizer. One measurement of the counting efficiency for solid particles derives that APS has 85% to 100% counting efficiency. The detailed descriptions on these instruments were summarized in Table 2. Simultaneous measurement of them revealed that number concentration reported by the PDM was lower in the comparable range than the APS in polydisperse

Table 2. Particle counter specification.

| | Grimm PDM 1108 | TSI APS 3320 |
|-------------------------------------|----------------|----------------------------|
| Measurement principal | Optical | Optical and Time-of-flight |
| Size range, μm | 0.3-20 | 0.5-20 |
| Number of channels | 15 | 52 |
| Max number conc. p cm^{-3} | 2,000 | 1,000 |
| Max mass conc. mg m^{-3} | 100 | Not reported |

**Fig. 3.** The result of simultaneous measurements with APS and PDM ((a) size distribution, (b) total number concentration).

test while the PDM was greater than the APS in mono-disperse tests. In this study, the simultaneous measurements of APS and PDM in the same condition also revealed a similar trend to the previous works as shown in Fig. 3. In spite of a little underestimation of PDM, the correlation coefficient (0.99) between the two instruments is sufficiently high. An evaluation of the model 3320 APS also showed that the particle recirculation in the optics region caused by the shape of education nozzle could lead to false large-particle counts in APS 3320, and the side scatter by these missed particles mainly observed in the large size range, more than $10 \mu\text{m}$ (Stein *et al.*, 2002).

RH uncertainty was calculated from the difference between collocated measurements of the RH on the sheath and inlet flows of nephelometer. A regression between RH sheath and RH sample gives a slope of 0.96, and offset of 5.6% and R^2 of 0.81. The average magnitude of the difference in RH measurements for the sample and sheath flows was 2.50 ± 6.08 in % RH units for $n=468$ samples (removing 1 outliers and precipitation periods).

Optec NGN integrating nephelometers were operated in various configurations (Malm *et al.*, 2005a; Day *et al.*, 2000; Molenaar, 1997). In this study, the Optec-derived $\text{PM}_{2.5}$ scattering coefficients were compared

with the TSI model 3563 data for TSP in order to validate the measured data. At this time, the TSI-derived scattering values of $\text{PM}_{2.5}$ were calculated by using the number concentration of coarse particle measured by APS and IMPROVE equation for estimating the ambient scattering of coarse particles. As a result, the $\text{PM}_{2.5}$ scattering coefficients measured by OPTEC and TSI nephelometers show good correlation ($R=0.93$) and have a slope of 0.89. The average magnitude of difference in two instruments was 7.4 Mm^{-1} (removing 9 outliers and precipitation periods), and it is ranged in the reasonable error which could be caused by the calculation of $\text{PM}_{2.5}$ scattering from TSI-derived TSP values as well as monitoring condition such as the location and structure of sampling inlet.

System performance was also tested during the intensive field campaign by simultaneous measuring the scattering coefficients without diffusion scrubber for 24 hours. As a result, the correlation coefficient between two parallel systems was 0.98 and the slope was 0.99 indicating the equivalence of two parallel systems.

3.2 Overview of Optical Properties of $\text{PM}_{2.5}$ during ABC-EAREX 2005

The air quality offered by the Korean Ministry of

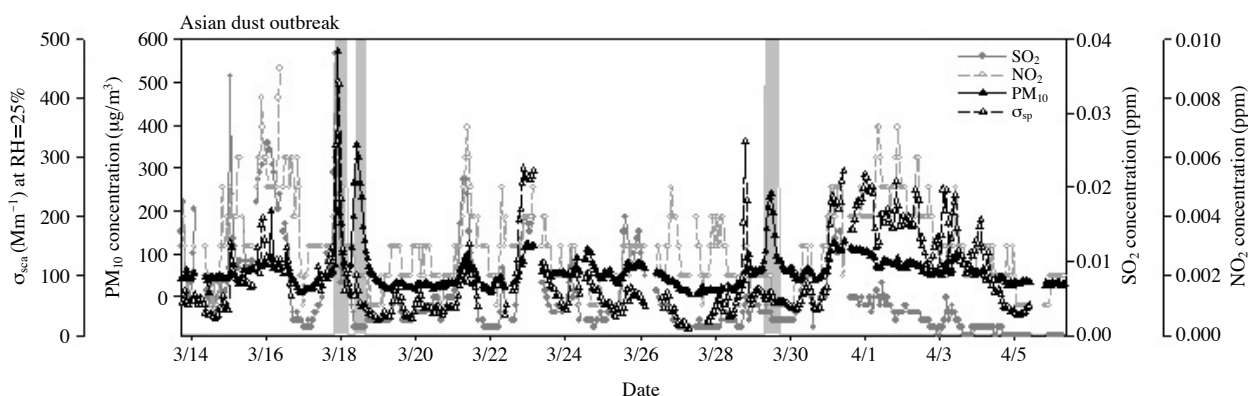


Fig. 4. Temporal variation of air quality at Gosan during ABC-EAREX 2005.

Table 3. Chemical composition of fine aerosol classified by RH.

| | RH (%) | | | | | | Total |
|-------------------------------|---------------|---------------|---------------|---------------|---------------|-------------|-------------|
| | 80 ≤ RH < 90% | 70 ≤ RH < 80% | 60 ≤ RH < 70% | 50 ≤ RH < 60% | 40 ≤ RH < 50% | RH < 40% | |
| Mass | 25.2 ± 16.4 | 46.6 ± 23.8 | 30.4 ± 16.1 | 27.9 ± 23.7 | 22.6 ± 10.2 | 22.8 ± 9.1 | 29.6 ± 19.2 |
| Cl ⁻ | 0.54 ± 0.21 | 0.65 ± 0.27 | 0.77 ± 0.35 | 0.90 ± 0.72 | 0.77 ± 0.40 | 0.67 ± 0.29 | 0.76 ± 0.48 |
| SO ₄ ²⁻ | 4.79 ± 4.57 | 8.57 ± 4.61 | 5.99 ± 4.43 | 4.14 ± 3.8 | 3.24 ± 1.68 | 2.38 ± 1.20 | 5.14 ± 4.27 |
| NO ₃ ⁻ | 1.62 ± 1.03 | 3.20 ± 2.33 | 2.39 ± 2.15 | 1.48 ± 1.90 | 1.17 ± 0.98 | 0.92 ± 0.48 | 1.92 ± 1.98 |
| Na ⁺ | 0.30 ± 0.16 | 0.41 ± 0.13 | 0.42 ± 0.15 | 0.44 ± 0.19 | 0.39 ± 0.14 | 0.35 ± 0.13 | 0.40 ± 0.16 |
| NH ₄ ⁺ | 2.20 ± 0.92 | 3.31 ± 1.71 | 2.16 ± 1.48 | 1.39 ± 1.41 | 1.10 ± 0.92 | 0.73 ± 0.48 | 1.88 ± 1.56 |
| K ⁺ | 0.26 ± 0.11 | 0.38 ± 0.13 | 0.32 ± 0.11 | 0.30 ± 0.13 | 0.31 ± 0.09 | 0.30 ± 0.12 | 0.32 ± 0.12 |
| Mg ²⁺ | 0.05 ± 0.02 | 0.07 ± 0.03 | 0.07 ± 0.04 | 0.09 ± 0.05 | 0.07 ± 0.04 | 0.08 ± 0.04 | 0.08 ± 0.04 |
| Ca ²⁺ | 0.14 ± 0.05 | 0.17 ± 0.09 | 0.16 ± 0.08 | 0.24 ± 0.16 | 0.22 ± 0.21 | 0.23 ± 0.14 | 0.20 ± 0.14 |
| OC | 3.55 ± 0.91 | 4.95 ± 1.64 | 4.25 ± 1.79 | 3.86 ± 1.92 | 3.54 ± 1.32 | 3.43 ± 1.55 | 4.03 ± 1.73 |
| EC | 0.97 ± 0.71 | 1.84 ± 0.91 | 1.32 ± 0.79 | 1.20 ± 0.80 | 1.00 ± 0.54 | 0.84 ± 0.39 | 1.26 ± 0.81 |

Environment and optical properties obtained during the entire field campaign are shown in Fig. 4. The measured dry σ_{sp} values ranged from 9.0 to 430 Mm^{-1} with an average period of about 99 Mm^{-1} over the whole. The average values are comparable to σ_{sp} values obtained in the regions influenced by anthropogenic emissions like the continental boundary layers during INDOEX (85 Mm^{-1}) and the Negev Desert in Israel during ARACHNE (90 Mm^{-1}) (Mayol-Bracero *et al.*, 2002; Formenti *et al.*, 2001). Especially, the very high value of σ_{sp} , more than 250 Mm^{-1} , was only observed during the initial stage of AD phenomena (73.9–430 Mm^{-1}) and heavy pollution periods (149–282 Mm^{-1}), and the maximum value is comparable with 410 Mm^{-1} for a day with heavy smog reported in Los Angeles, California, USA (Seinfeld and Pandis, 1998). For clear days when the $PM_{2.5}$ mass concentration was lower than 30 $\mu g/m^3$, the scattering coefficient was about 54 Mm^{-1} and ranged from 9.0 to 139 Mm^{-1} , which is similar to the typical value of moderately polluted continental air masses such as the mid-Atlantic coast of the US during TARFOX (53–196

Mm^{-1}) and the continental air masses studied during ACE-2 (0.11–100 Mm^{-1}) (Quinn *et al.*, 2000; Hegg *et al.*, 1997).

3.3 Average Chemical Composition of Fine Aerosol in Different RH Condition

Generally, water vapor may be absorbed and condensed on hydrophilic aerosols when the atmospheric RH is increased. The aerosol water uptake changes the particle size as well as the optical properties of ambient aerosol. As shown in Table 3, the concentrations of several ionic species such as sulphate, nitrate, and ammonium as well as carbonaceous materials in $PM_{2.5}$ were obviously increased according to the elevation of RH when RH values were less than 80%. Especially, the concentrations of sulphate, nitrate, and ammonium in the RH range from 70% to 80% were 3.5, 3.6, and 4.6 times higher than those in low RH values (<40%), respectively. However, when RH is higher than 80%, the concentration of hydrophilic chemical components in $PM_{2.5}$ decreased implying that the excessively damp air makes particles grow

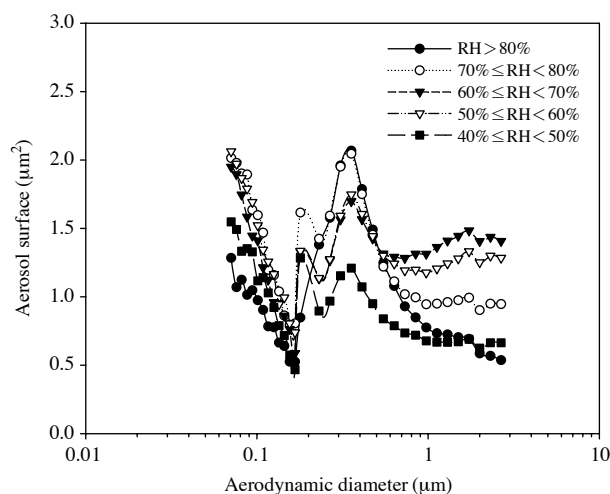


Fig. 5. Average size distribution in ambient condition classified by RH.

into a coarse one, more than $2.5 \mu\text{m}$. In particular, the steep decrease of fine mass, about 50% than that in the range $70\% < \text{RH} < 80\%$, implies that fine particles in high RH condition ($> 80\%$) may be diminished by the sudden hygroscopic growth as well as the adhesion into the coarse one.

3.4 Cross-sectional Area Distributions as a Function of RH

Size distributions of particulate surface area are compared in different RH ranges in order to study the influence of high RH and water uptake on aerosol size distribution. The average size distribution classified by RH in the fine size range ($D_p < 2.5 \mu\text{m}$) reveals that the particulate surface area increases according to the RH elevation when RH was less than 80%. Especially, the increase of surface area was mainly observed in the droplet mode, around $0.6 \mu\text{m}$, as shown in Fig. 5. However, when humidity is ramped to high RH values ($> 80\%$), the aerosol surface in the droplet mode was not increased in the same way with the concentration of hydrophilic species in $\text{PM}_{2.5}$ implying that the hygroscopic growth of particles mainly occurred in the coarse size range, larger than $2.5 \mu\text{m}$.

In order to see the hygroscopic growth in the coarse size range ($D_p > 2.5 \mu\text{m}$) with RH exceeding 80%, size distribution of surface areas in a wider size range of $0.07\text{--}17 \mu\text{m}$ was compared between in normal and dry conditions. Fig. 6 shows that the particulate surface area in high ambient RH condition ($> 80\%$) and the difference of them between in normal and dry conditions are steeply increased when the aerodynamic diameter is larger than $10 \mu\text{m}$. Although the size distribution measured by APS 3320 was not calibrated

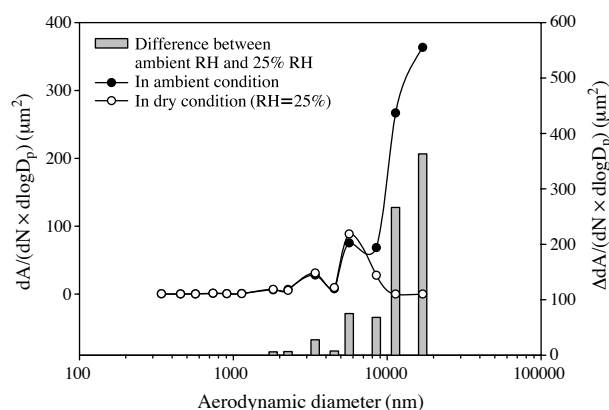


Fig. 6. Comparison of particulate surface distribution in ambient and dry condition (RH=25%).

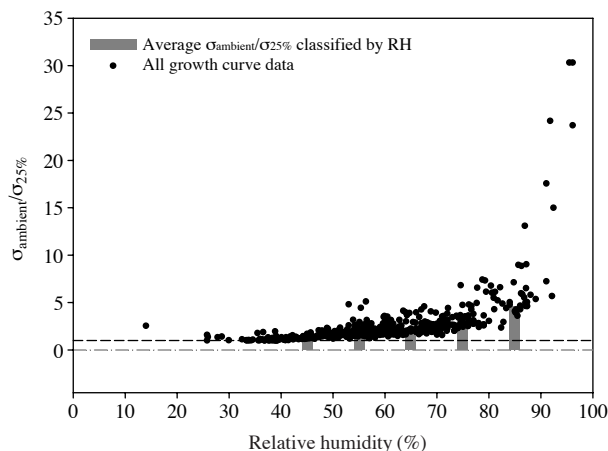
in the coarse size range by using the correlated mask, the large amount of difference in surface area definitely shows that most hygroscopic growth of aerosol occurred in the coarse particles ($D_p > 10 \mu\text{m}$) when RH was higher than 80%. Moreover, the graph reveals that the surface area in the droplet mode was lower in the normal condition than in the dry condition, suggesting that fine aerosol in the droplet mode could be grown to that in the coarse mode in the high RH condition ($> 80\%$) by the physical interaction between particles such as adhesion or coagulation. This fact well describes the decrease of mass and inorganic salts in fine aerosol when RH is higher than 80%.

3.5 Variation of Scattering Coefficients according to the Atmospheric RH

Particulate matter is a mixture of components that are formed by a wide variety of mechanisms associated with both natural and anthropogenic origins (Alves *et al.*, 2001). Especially, atmospheric sulfates are often found to be associated with the fine particulate mass, in the size range from $0.1 \mu\text{m}$ to $1.0 \mu\text{m}$, where particles can most efficiently scatter sunlight. Therefore, a strong correlation between light scattering and sulphate mass concentration has been observed (Tang, 1996; White, 1976). The inorganic salt aerosols including sulfate are mostly hygroscopic in nature and exhibit the property of deliquescence in humid air (Tang, 1980). Therefore, the optical properties of aerosol such as scattering and absorbing properties could be modified by RH (Chazette and Lioussé, 2001). The scattering coefficients (σ_{sca}) and the number concentrations (dN) of fine aerosol ($D_p < 2.5 \mu\text{m}$) classified by RH ranges are shown in Table 4. Overall, they reveal the largest values when RH is ranged from 70% to 80%, similar to the concentration of sulphate, nitrate, and carbonaceous materials. On the other hand, the ratios

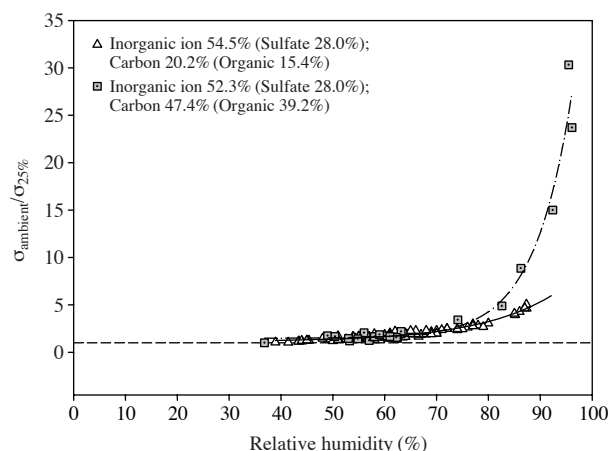
Table 4. Statistical summary of scattering coefficient and number concentration of fine aerosol in selective RH ranges.

| | $\sigma_{\text{sca, ambient}}$ (Mm^{-1}) | $\sigma_{\text{sca, 25\%}}$ (Mm^{-1}) | dN_{ambient} | $dN_{25\%}$ | $\Delta\sigma_{\text{sca}}$ | $\sigma_{\text{scat, ambient}}/\sigma_{\text{scat, 25\%}}$ |
|----------------------------|--|---|-----------------------|---------------|-----------------------------|--|
| RH < 40% | 27.6 ± 7.8 | 24.2 ± 7.2 | 81 ± 28 | 91 ± 28 | 3.35 | 1.17 ± 0.25 |
| $40 \leq \text{RH} < 50\%$ | 43.9 ± 22.4 | 30.8 ± 12.3 | 131 ± 73 | 121 ± 53 | 13.10 | 1.44 ± 0.29 |
| $50 \leq \text{RH} < 60\%$ | 76.1 ± 50.4 | 39.6 ± 28.4 | 169 ± 138 | 159 ± 124 | 36.51 | 2.00 ± 0.64 |
| $60 \leq \text{RH} < 70\%$ | 113.4 ± 61.4 | 52.0 ± 32.5 | 226 ± 152 | 227 ± 155 | 61.34 | 2.34 ± 0.67 |
| $70 \leq \text{RH} < 80\%$ | 234.8 ± 118.6 | 78.8 ± 38.9 | 377 ± 187 | 347 ± 187 | 156.04 | 3.16 ± 1.21 |
| $80 \leq \text{RH} < 90\%$ | 229.7 ± 151.4 | 43.0 ± 30.2 | 227 ± 159 | 194 ± 139 | 179.49 | 4.58 ± 1.59 |

**Fig. 7.** Scattering plot of hygroscopic factor data at Gosan during ABC-EAREX 2005.

of $\sigma_{\text{scat, ambient}}/\sigma_{\text{scat, 25\%}}$ was increased corresponds to the elevation of RH in the whole RH ranges. In spite of the reduction of scattering coefficients and number concentration of $\text{PM}_{2.5}$, the sharp increase of the ratio in the high RH range ($80\% \leq \text{RH} < 90\%$) could be caused by the phase transformation from a solid particle to a droplet. Generally, the phase transformation usually occurs spontaneously when the relative humidity in the surrounding atmosphere reaches a level, known as the deliquescence point that is specific to the chemical composition of the aerosol article (Tang and Munkelwitz, 1993; Tang, 1976). The phase transformation as a function of the relative humidity was clearly indicated at about 80% RH for $(\text{NH}_4)_2\text{SO}_4$ and at 75% RH for NaCl (Tang, 1996; Tang and Munkelwitz, 1993).

Fig. 7 shows the deliquescent behavior of ambient aerosol at Gosan during ABC-EAREX 2005. The plot shows the influence of RH on the aerosol water uptake. Overall, growth curve data made a similar appearance with the general shape of the compilation growth curves. Especially, the growth curve indicates that the aerosol appeared to start absorbing some water somewhere between 45% and 60% RH with the average ratios of $\sigma_{\text{scat, ambient}}/\sigma_{\text{scat, 25\%}}$ 1.10 for 40% RH, 1.11

**Fig. 8.** Growth curve structures for subdivided periods representative of different chemical compositions.

for 50% RH, and 1.17 for 60% RH, respectively. It is considerably different with that at Great Smoky where a smooth and continuous growth above 20% RH while the deliquescent points were similar with Grand Canyon (Day and Malm, 2001).

3.6 Relationship between Hygroscopicity and Chemical Composition

In order to investigate the influence of chemical components on the hygroscopic growth, the average chemical composition and the corresponding growth curves were studied. Fig. 8 shows the average chemical composition and the corresponding growth curve for subdivided periods including when one of the lowest growth curves were measured and when one of the highest growth curves were measured at Gosan during ABC-EAREX 2005. When organic carbon and soluble inorganic compounds contributed 15% and 55% of the fine aerosol mass, respectively, there were very little uptake of water. On the other hand, the aerosol water uptake was much greater when there was about two times larger organic mass fraction and similar soluble inorganic fraction. This result suggests that the organic materials significantly contribute to water uptake during these studies. It is remarkably different with

the result of other previous studies in which they described that organic materials in TSP can suppress the water uptake of aerosol (Carrico *et al.*, 2005; Malm *et al.*, 2005b). For example, McInnes *et al.* (1998) has suggested that organic carbon may suppress water uptake by ambient aerosol (TSP) in a marine environment: A comparison of chemical composition and aerosol growth curves shows that the largest growth curves occur when the fractions of inorganic salts were highest. When the fractions of organic carbon and soil were high, the growth curves were lower. Brooks *et al.* (2004) and Prenni *et al.* (2003) found that mixing organic aerosols with inorganic species showed a slightly depressed deliquescence point compared with the pure inorganic species within the uncertainty of the measurement. Especially, carboxylic acids and alkanes are known to decrease the amount of hygroscopic growth when those compounds replaced the inorganic compounds such as NaCl and $(\text{NH}_4)_2\text{SO}_4$ (Choi and Chan, 2002; Hansson *et al.*, 1998). Reduction of hygroscopic growth was also caused by the increasing mass fraction of organic material for aerosols emitted from biomass burning (Carrico *et al.*, 2005; Malm *et al.*, 2005b). On the other hand, Saxena *et al.* (1995) described that the freshly produced organic carbon in an urban area (Los Angeles, CA) has a net effect of diminishing water content, while aged, that is, oxidized organic carbon in a rural setting (Grand Canyon, AZ) has a net effect of increasing the water content of the ambient aerosol.

It suggests that these dissimilar results on the water uptake by organic compounds could be caused by not considering the hygroscopic growth in the fine size ranges, the oxidation degree of organic matter, and the mixed state of organic matter with inorganic components. Generally, secondary aerosols containing sulfate, nitrate, ammonium, and various organic materials occupy the great portions of sub-micron aerosols. Therefore, the correlation between the hygroscopicity and the concentration of organic matters in the fine size range ($D_p < 2.5 \mu\text{m}$) can suggest how the oxidized organic ones contribute to the hygroscopic growth. In addition, the parallel system used in this study directly provides the information on optical and hygroscopic properties of ambient aerosol while the TDMA system can make the mixed structure of chemical components change during drying and humidification of ambient aerosol.

The hygroscopic growth curves of aerosol with the different composition of organic carbon are compared in Fig. 8. A comparison of chemical composition and aerosol growth curves shows that the increase in hygroscopic growth can be obtained when the fractions of organic carbon is high. Especially, the similar mass

fractions of inorganic salts in two cases imply that the difference of hygroscopic growth can be caused by the composition of carbonaceous materials. This suggests that particulate carbon compounds collected at Gosan, Korea are sufficiently aged and contribute as much as inorganic salts to aerosol water uptake. It is different from a previous work conducted by Kim *et al.* (2006) during ACE-Asia. The distinctive result can be caused by the difference of monitoring method, aerosol size range and so on. In addition, the relationship between hygroscopic growth and organic carbon has to be investigated under the consideration of the composition of inorganic salts.

4. SUMMARY AND CONCLUSIONS

High atmospheric RH causes the hygroscopic growth of ambient aerosol as well as the change of chemical composition, size distribution, and optical properties of it. Ambient fine aerosols ($D_p < 2.5 \mu\text{m}$) collected at Gosan, Korea during ABC-EAREX 2005 was dominated by water-soluble ionic species (35%) and carbonaceous materials (18%). Surface area distribution of aerosol shows that the elevation of RH makes the ambient aerosol grow to be the droplet mode around $0.6 \mu\text{m}$ and coarse mode, larger than $2.5 \mu\text{m}$. The hygroscopic growth was mainly observed in a larger size range of over $10 \mu\text{m}$. However, when RH is lower than 80%, the increase of droplet mode area was apparently observed in fine size range ($D_p < 2.5 \mu\text{m}$). The decrease of fine mass and scattering coefficients in high RH values also implies that the hygroscopic growth could make the fine aerosol grow to be the coarse one in extremely damp air ($\text{RH} > 80\%$) by the influence of the physical interaction between ambient particles such as the adhesion and coagulation.

The hygroscopic factor of ambient aerosol was calculated from the measured scattering coefficients at a given ambient RH and a reference RH (25%) using a parallel monitoring system. The result shows that water uptake began at intermediate RH range, from 40% to 60%. Average chemical composition and the corresponding growth curves were analyzed in order to investigate the relationship between carbonaceous material fraction and hygroscopicity. As a result, the positive relationship between carbonaceous material fraction and hygroscopicity was observed suggesting that carbonaceous components also contribute as much as water soluble ionic species to the aerosol water uptake at the Gosan super site. Moreover, it implies that the carbon components of $\text{PM}_{2.5}$ at Gosan could be sufficiently aged and made into a hydrophilic material by the oxidation in the atmosphere.

This result shows that the hygroscopic properties of ambient fine particles collected at Gosan during ABC-EAREX 2005 were significantly different with those of TSP and PM₁₀ studied in several previous works. The hygroscopic growth of fine aerosol was dominated by the growth of droplet mode aerosol, around 0.6–0.7 μm. Especially, the hygroscopic behaviour of the droplet mode particles was definitely different with the coarse mode ones. The results of this study suggest that the hygroscopic growth of fine aerosol can be mainly impacted by the organic carbon fraction. The large fraction of particulate organic materials could accelerate the formation of haze when fine carbonaceous aerosol is sufficiently oxidized during long range transportation, especially in the moderately humidified environment (RH < 80%).

REFERENCES

- Alves, C., Pio, C., Duarte, A. (2001) Composition of extractable organic matter of air particles from rural and urban Portuguese areas. *Atmospheric Environment* 35, 5485–5496.
- Arhami, M., Thomas, K., Fine, M.R., Delfino, J., Sioutas, C. (2006) Effects of sampling artifacts and operating parameters on the performance of a semicontinuous particulate elemental carbon/organic carbon monitor. *Environmental Science & Technology* 40, 945–954.
- Brechtel, F.J., Kreidenweis, S.M. (2000) Predicting particle critical supersaturation from hygroscopic growth measurement in the humidified TDMA: Part II: laboratory and ambient studies. *Journal of Atmospheric Sciences* 57, 1872–1887.
- Brooks, S.D., DeMott, P.J., Kreidenweis, S.M. (2004) Water uptake by particles containing humic materials and mixtures of humic materials with ammonium sulfate. *Atmospheric Environment* 38, 1859–1868.
- Carrico, C.M., Kreidenweis, S.M., Malm, W.C., Day, D.E., Lee, T., Carrillo, J., McMeeking, G.R., Collett, J.L. (2005) Hygroscopic growth behaviour of a carbon-dominated aerosol in Yosemite National Park. *Atmospheric Environment* 39, 1393–1404.
- Chazette, P., Liousse, C. (2001) A case study of optical and chemical ground apportionment for urban aerosols in Thessaloniki. *Atmospheric Environment* 35, 2497–2506.
- Choi, M.Y., Chan, C.K. (2002) The effects of organic species on the hygroscopic behaviours of inorganic aerosols. *Environmental Science & Technology* 36, 2422–2428.
- Day, D.E., Malm, W.C., Kreidenweis, S.M. (2000) Aerosol light scattering measurements as a function of relative humidity. *Journal of the Air & Waste Management Association* 50, 710–716.
- Day, D.E., Malm, W.C. (2001) Aerosol light scattering measurements as a function of relative humidity: a comparison between measurements made at three different sites. *Atmospheric Environment* 35, 5169–5176.
- Dick, W.D., Saxena, P.H., McMurry, P.H. (2000) Estimation of water uptake by organic compounds in sub-micron aerosols measured during the southeastern aerosol and visibility study. *Journal of Geophysical Research* 105, 1471–1479.
- Formenti, P., Andreae, M.O., Andreae, T.W., Ichoku, C., Schebeske, G., Kettle, A.J., Maenhaut, W., Cafmeyer, J., Ptasinaky, J., Karnieli, A., Lelieveld, J. (2001) Physical and chemical characteristics of aerosols over the Negev Desert (Israel) during summer 1996. *Journal of Geophysical Research* 106, 4871–4890.
- Han, J.S., Moon, K.J., Ahn, J.Y., Hong, Y.D., Kim, Y.J., Ryu, S.Y., Cliff, S.S., Cahill, T.A. (2004) Characteristics of ion components and trace elements of fine particles at Gosan, Korea in spring time from 2001 to 2002. *Environmental Monitoring and Assessment* 92, 73–93.
- Han, J.S., Moon, K.J., Lee, S.J., Kim, Y.J., Ryu, S.Y., Cliff, S.S., Yi, S.M. (2006) Size-resolved source apportionment of ambient particles by positive matrix factorization. *Atmospheric Chemistry and Physics* 6, 211–223.
- Han, J.S., Moon, K.J., Kim, Y.J. (2006a) Identification of potential sources and source regions of fine ambient particles measured at Gosan background site in Korea using advanced hybrid receptor model combined with positive matrix factorization. *Journal of Geophysical Research* 111, D22217, doi:10.1029/2005JD006577.
- Han, J.S., Moon, K.J., Hong, Y.D., Kondo, Y., Miyazaki, Y., Kim, Y.J. (2006b) Validation of PM_{2.5} carbon measurement protocols for semi-continuous carbon monitor, Proceedings of the seventh International Aerosol Conference (IAC), edited by P. Biswas, D. Chen, and S. Hering, pp. 534–535, AAAR, St. Paul, Minnesota, USA.
- Hansson, H.C., Rood, M.J., Koloutsou-Vakakis, S., Hameiri, K., Orsini, D., Wiedensohler, A. (1998) NaCl aerosol particle hygroscopicity dependence on mixing with organic compounds. *Journal of Atmospheric Chemistry* 31, 321–346.
- Hegg, D.A., Livingston, J., Hobbs, P.V. (1997) Chemical apportionment of aerosol column optical depth off the Mid-Atlantic Coast of the United States. *Journal of Geophysical Research* 102, 25,293–25,303.
- Kim, J., Yoon, S.C., Jefferson, A., Kim, S.W. (2006) Aerosol hygroscopic properties during Asian dust, pollution, and biomass episodes at Gosan, Korea in April 2001. *Atmospheric Environment* 40, 1550–1560.
- Malm, W.C., Day, D.E., Carrico, C., Kreidenweis, S.M., Collett Jr., J.L., McMeeking, G., Lee, T., Carrillo, J., Schichtel, B. (2005a) Intercomparison and closure calculations using measurements of aerosol species and optical properties during the Yosemite Aerosol Characterization Study. *Journal of Geophysical Research* 110, D14302, doi:10.1029/2004JD005494.
- Malm, W.C., Day, D.E., Kreidenweis, S.M., Collett Jr.,

- J.L., Carrico, C., McMeeking, G., Lee, T. (2005b) Hygroscopic properties of an organic-laden aerosol. *Atmospheric Environment* 39, 4969-4982.
- Mayol-Bracero, O.L., Gabriel, R., Andreae, M.O., Kirchstetter, T.W., Novakov, T., Ogren, J., Sheridan, P., Streets, D.G. (2002) Carbonaceous aerosol over the Indian Ocean during the Indian Ocean Experiment (INDOEX): Chemical characterization, optical properties, and probable sources. *Journal of Geophysical Research* 107 (D19), doi: 10.1029/2000JD000039.
- McInnes, L., Bergin, M., Ogren, J. (1998) Apportionment of light scattering and hygroscopic growth to aerosol composition. *Geophysical Research Letters* 25, 513-516.
- McMurry, P.H., Stolzenburg, M.R. (1998) On the sensitivity of particle size to relative humidity for Los Angeles aerosols. *Atmospheric Environment* 23(2), 497-507.
- Molenaar, J.V. (1997) Analysis of the real world performance of the Optec NGN-2 ambient nephelometers, In: *Visual Air Quality: Aerosols and Global Radiation Balance*, Air & Waste Management Association, Pittsburgh, pp. 243-265.
- Moon, K.J., Han, J.S., Jung, I.R., Kondo, Y., Miyazaki, Y. (2006) Evaluation of a URG ambient ion monitoring system (AIM) for measuring water soluble ion components of ambient PM_{2.5}: Intercomparison with PILS-IC monitor, Proceedings of the seventh International Aerosol Conference (IAC), edited by P. Biswas, D. Chen, and S. Hering, pp. 416-417, AAAR, St. Paul, Minnesota, USA.
- Oberreit, D.R., Holm, R.L., Hairston, P.P., Quant, F.R., Sem, G.J. (2001) Improvements in Particle Mass Distribution measurement with the TSI 3320 APS, poster paper presented at American Association for Aerosol Research Conference.
- Peterson, M.R., Richards, M.H. (2002) Thermal-Optical-Transmittance Analysis for Organic, Elemental, Carbonate, Total Carbon, and OCX₂ in PM_{2.5} by the EPA/NIOSH Method, RTI International conference proceeding, 19 pp., Research Triangle Institute, Washington, D.C., USA.
- Prenni, A.J., Demott, P.J., Kredenweis, S.M. (2003) Water uptake of internally mixed particles containing ammonium sulfate and dicarboxylic acids. *Atmospheric Environment* 37, 4243-4251.
- Quinn, P.K., Bates, T.S., Coffman, D.J., Miller, T.L., Johnson, J.E., Covert, D.S., Putaud, J.P., Neusub, C., Novakov, T. (2000) A comparison of aerosol chemical and optical properties from the 1st and 2nd Aerosol Characterization Experiments. *Tellus, Ser. B*, 52, 239-257, 2000.
- Quinn, P.K., Coffman, D.J., Bates, T.S., Miller, T.L., Johnson, J.E., Welton, E.J., Neususs, C., Miller, M., Sheridan, P.J. (2002) Aerosol optical properties during INDOEX 1999: Means, variability, and controlling factors. *Journal of Geophysical Research* 107(D19), 8020, doi: 10.1029/2000JD000037.
- Ramanathan, V., Crutzen, P.J., Lelieveld, J., Mitra, A.P., Althausen, D., Anderson, J., Andreae, M.O., Cantrell, W., Cass, G.R., Chung, C.E., Clarke, A.D., Coakley, J.A., Collins, W.D., Conant, W.D., Dulac, F., Heintzenberg, J., Heymsfield, A.J., Holben, B., Howel, S., Hudson, J., Jayaraman, A., Kiehl, J.T., Krishnamurti, T.N., Lubin, D., McFarquhar, G., Novakov, T., Ogren, J.A., Podgorny, I.A., Prather, K., Priestley, K., Prospero, J.M., Quinn, P.K., Rajeev, K., Rasch, P., Rupert, S., Sadourny, R., Satheesh, S.K., Shaw, G.E., Sheridan, P., Valero, F.P.J. (2001) Indian Ocean Experiment: An integrated analysis of the climate forcing and effects of the great Indo-Asian haze. *Journal of Geophysical Research* 106, 28371.
- Ramanathan, V., Crutzen, P.J. (2003) New Directions: Atmospheric Brown "Cloud". *Atmospheric Environment* 37, 4033-4035.
- Saxena, P., Hildemann, L.M., McMurry, P.H., Seinfeld, J.H. (1995) Organics alter hygroscopic behaviour of atmospheric particles. *Journal of Geophysical Research* 100, 18755-18770.
- Seinfeld, J.H., Pandis, S.N. (1998) *Atmospheric chemistry and physics from air pollution to climate change*, pp. 901-912, John Wiley & Sons, Inc., New York, USA.
- Sisler, J.F., Malm, W.C. (2000) Interpretation of trends of PM_{2.5} and reconstructed visibility from the IMPROVE network. *Journal of Air & Waste Management Association* 50, 775-789.
- Stein, S.W., Gabrio, B.J., Oberreit, D.R., Hairston, P.P., Myrdal, P.B., Beck, T.J. (2002) An evaluation of mass-weighted size distribution measurements with the model 3320 Aerodynamic Particle Sizer. *Aerosol Science and Technology* 36, 845-854.
- Swietlicki, E., Zhou, J., Berg, O.H., Martinsson, B.G., Goran, F., Cederfelt, S., Dusek, U., Berner, A., Birmili, W., Wiendensohler, A., Yuskiewicz, B., Bower, K.N. (1999) A closure study of sub-micrometer aerosol particle hygroscopic behaviour. *Atmospheric Research* 50, 205-240.
- Tang, I.N. (1976) Phase transformation and growth of aerosol particles composed of mixed salts. *Journal of Aerosol Science* 7, 361-371.
- Tang, I.N. (1980) Deliquescence properties and particle size change of hygroscopic aerosols, in *Generation of Aerosols*, edited by K. Willeke, chap. 7, Butterworth, Stoneham, Mass.
- Tang, I.N., Munkelwitz, H.R. (1993) Composition and temperature dependence of the deliquescence properties of hygroscopic aerosols. *Atmospheric Environment* 27A, 467-473.
- Tang, I.N. (1996) Chemical and size effects of hygroscopic aerosols on light scattering coefficients. *Journal of Geophysical Research* 101(D14), 19245-19250.
- White, W.J. (1976) Reduction of visibility by sulfate in photochemical smog. *Nature* 264, 735-736.